https://doi.org/10.1016/j.tre.2021.102427

An improved learning-and-optimization train fare design method for addressing commuting congestion at CBD stations

Submitted by

Xinyuan Chen, Ph.D., Lecturer
College of Civil Aviation, Nanjing University of Aeronautics and Astronautics, China
Department of Logistics and Maritime Studies, The Hong Kong Polytechnic University,
Hung Hom, Kowloon, Hong Kong, China
E-mail: xinyuan.chen@polyu.edu.hk

Wei Zhang, Research assistant professor
Department of Logistics and Maritime Studies, The Hong Kong Polytechnic University,
Hung Hom, Kowloon, Hong Kong, China
E-mail: wei.sz.zhang@connect.polyu.hk

Xiaomeng Guo, Ph.D., Assistant professor
Department of Logistics and Maritime Studies, The Hong Kong Polytechnic University,
Hung Hom, Kowloon, Hong Kong, China
E-mail: xiaomeng.guo@polyu.edu.hk

Zhiyuan Liu, Ph.D., Professor
Jiangsu Key Laboratory of Urban ITS, Jiangsu Province Collaborative Innovation Center of Modern Urban Traffic Technologies, School of Transportation, Southeast University, China
E-mail: zhiyuanl@seu.edu.cn

AND

Shuaian Wang, Ph.D., Associate professor
Department of Logistics and Maritime Studies, The Hong Kong Polytechnic University,
Hung Hom, Kowloon, Hong Kong, China
E-mail: wangshuaian@gmail.com

Corresponding Author:
Shuaian Wang

July, 2021

An improved learning-and-optimization train fare design method for addressing commuting congestion at CBD stations

Abstract

This study proposes an improved learning-and-optimization train fare design method to deal with the commuting congestion of train stations at the central business district (CBD). The conventional learning-and-optimization scheme needs accurate boarding/alighting demand to update the train fare in each trial. However, when congestion happens, the observed boarding/alighting demand will be larger than the actual boarding/alighting demand due to the delays and the longer dwelling time. Thus, the actual boarding/alighting demand is not available in practice. The improved algorithm deals with this issue by using inexact and less information to determine the new trial fare during the iteration. Namely, the improved method bypasses the conditions that may lead to biased results so as to significantly enhance the reliability of the learning-and-optimization method. The simplified algorithm also makes this method more practical. The convergence property of the proposed algorithm is rigorously proved and the convergence rate is demonstrated to be exponential. Numerical studies are performed to demonstrate the efficiency of the improved learning-and-optimization method.

Keywords: learning-and-optimization, commuting congestion management, train fare design, bi-objective optimization

1 Introduction

Train, service capacity of which is much larger than other transport modes, is one of the dominant modes in the urban transport system for commuting purposes, especially in megacities, such as Sydney, New York, and London. In Sydney, approximately 320 thousand commuters alight at major destination locations (i.e., CBD train stations) every day with an average 16.5 km commuting distance (Australian Bureau of Statistics, 2018; Wang et al., 2018). The high commuting volume occurs at morning/afternoon peak hours and results in commuting congestion (i.e., boarding/alighting congestion) on train station platforms where the passengers obstruct each other to get on/off trains due to limited walking spaces.

The commuting congestion makes dwell time increase sharply at CBD stations. The train must be stopped for a much longer time to let passengers get on/off and in the meantime, the following trains have to stay in the upstream stations to wait for the pass-signal of the downstream blocked train, since they utilize the same infrastructure. Train services are not as flexible as private vehicles, which means one blocked train reduces the headway of the following trains and then, and limit the total system service capacity of the whole train service system. Several approaches are considered to address this problem, such as (1) improving the service capacity of CBD stations; (2) shifting train travel demand to other transport modes; (3) adjust commuters' travel decisions over time. All of these approaches have limitations. The first approach is a long-term investment due to the large human and financial requirements. Thus, it is not available to retain the passenger demand to the designed/preplanned level in the short term. The second approach collides with the environmental-friendly commuting principle because train is much more efficient than most of the other modes in the aspect of pollutant emission. The third approach may also not be suitable for commuters who have to obey strictly restricted working hours.

To address the abovementioned issues, Wang et al. (2018) proposed an alternative approach to control the pedestrian demand of congested CBD train stations. Their approach is inspired by a real situation in Sydney, where four train stations at the same rail line in the CBD are close to each other. The middle two stations are nearest to shopping malls and office

buildings, which attract huge commuting travel demands to board/alight at these two stations and result in commuting congestions. Meanwhile, the other two train stations are uncongested and still have sufficient capacity to accommodate commuting travel demands. Currently, the time interval between two successive trains is 7 minutes during rush hours, while the train service frequency cannot be further increased because of the congestion at the bottleneck stations. The pedestrian distance between these neighboring stations ranges from 700 meters to 1100 meters, therefore, a part of travel demands can shift to adjacent uncongested train stations. Considering this situation, a potential approach to spread the excess demand at the middle two stations is imposing a different train fare scheme. Due to the train stations are very close, the difference in pedestrian distance is marginal. Figure 1 shows the general layout of train stations in this background. When increasing the train fare for commuting passengers at congested stations, i.e., station 1 and station 2, some passengers would shift to nearby stations. Namely, the passengers at station 1 may switch to station 0 and station 2, and the passengers at station 2 may switch to station 1 and station 3, depending on the fare charge pattern. To minimize the train fare increases at congested stations, a bi-objective mathematical programming model is built. Note that the exact expression of demand function (passengers' reaction to train fare increases) in this mathematical programming model is unknown. Considering the complexity of passengers' decision-making process (Gao et al., 2020; Qu et al., 2020; Wu et al., 2020; Xu et al., 2021), it is hard to precisely predict the response of passengers to the train fare adjustment. To address a mathematical optimization problem with unknown demand functions, Wang et al. (2018) designed a learning-and-optimization pricing algorithm (we use "algorithm 1" to refer to Wang et al. (2018)'s scheme and use "algorithm 2" to refer to the new scheme proposed in our paper), which guarantees the convergence of the toll charge without the exact demand function (Wang et al., 2018). The fare increases pattern is adjusted in a sequence of trials, in which each trial reveals some information about the commuters' response, and based on the accumulated information, the fare increases pattern could be iteratively adjusted until the optimal fare increases pattern is reached. The solution approach proposed by Wang et al. (2018) is an exact algorithm, rather than a heuristic algorithm

(Chu and Hsu, 2019; Kavoosi et al., 2019). The convergence of algorithm 1 is ensured by restricting the domain of the demand function, iteratively. In each iteration, according to the observation of passengers' responses, at least half of the domain can be removed. In other words, algorithm 1 has an exponential convergence rate. In this study, we notice that there exist two major limitations of algorithm 1 and propose an improved learning-and-optimization scheme that addresses the two limitations.

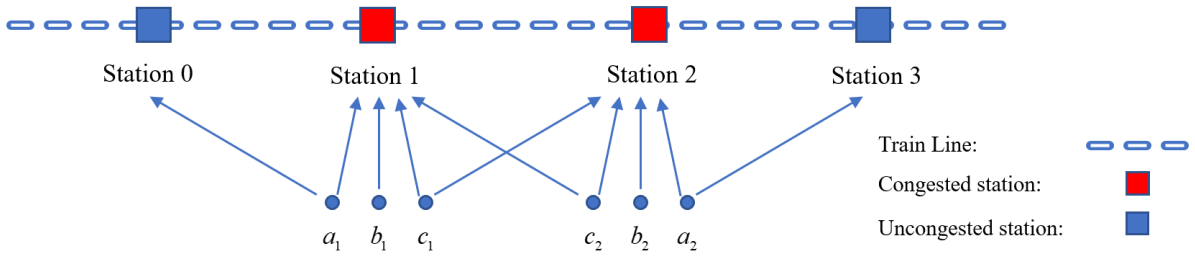

Figure 1 The train fare differentiation scheme to decentralize demands at congested stations.

First, it is hard to precisely observe the actual passenger demand at congested train stations during peak hours. Here, we define passenger demand as the measured volume of travel flow that is served by once train service which is determined by the dwelling time, the boarding/alighting rate, and the number of train doors. Actual passenger demand represents the boarding/alighting volume within preplanned dwelling time, while the observed passenger demand reflects the boarding/alighting volume within observed dwelling time. In algorithm 1, the train fare increases are adjusted by the observed passenger demand. In this study, we point out that the observed demand is not exactly equal to the actual passenger demand, in congestion scenarios. Although train carriages have sufficient capacity to accommodate passengers, the space between travelers will be significantly compressed and the excessively high demand will delay the boarding/alighting process, i.e., causing the commuting congestion. When such congestion happens, the train has to stay for a much longer period of time to let passengers board/alight. The longer dwelling time would further allow more passengers to arrive at the platform, board, and make the observed demand to be larger than the actual demand. What's more, as mentioned above, the following trains also have to stay in the upstream stations to wait for the pass signal of the downstream blocked train. During that period, more passengers

would board these upstream trains. When these trains carry excess passengers from the upstream stations to the downstream stations, it is inevitable to aggravate the congestion and stay longer to allow passengers boarding/alighting. Therefore, in congestion scenarios, the observed passenger demand should be larger than the actual demand, rather than equal to. When designing the train fare increases scheme, algorithm 1 requires the actual passenger demand to identify the infeasible pricing space. Algorithm 1 summarizes six scenarios that may happen after imposing an additional fare scheme. In these scenarios, except for the actual passenger demand, the total demand for two congested stations is also required. However, as we discussed, the passenger demand cannot be exactly estimated/observed. Overestimated passenger demand would magnify the train fare differences and result in zigzag fluctuation during the train fare adjustment process.

Second, algorithm 1 did not fully utilize the model's properties. The monotonicity of the demand function reveals that by increasing both fares at congested stations with the same amount, no passengers will shift between congested stations, but a few passengers will shift to uncongested nearby stations (details will be described in Property 2 in Section 3). We also know the monotonicity of the demand function. By using these two properties, we could still identify infeasible regions (details will be provided in Section 4) based on the trial scheme. That means the total demand for two congested stations in algorithm 1 is no longer needed in the improved algorithm. In this regard, we can use less information to ensure the convergence of the algorithm, to avoid using unreliable information and to improve the reliability of the proposed algorithm. In other words, the observed volume is not necessarily required, and we just need an indicator to show whether a train station is running over capacity or not. In addition, because less information is required, the six scenarios presented in algorithm 1 can be reduced into four scenarios which further simplifies the learning-and-optimization scheme and enhance its practicability. By choosing an appropriate trial scheme, we proved that at least half of the domain can be eliminated in each iteration. Thus, algorithm 2 could achieve the same convergence velocity as algorithm 1. In other words, with less information, the improved algorithm could still converge at an exponential rate.

In summary, this study is conducted to address the commuting congestion of two always congested stations in the CBD. A train fare differentiation scheme is imposed on four adjacent train stations to spread a part of commuters to the adjacent stations with sufficient capacity. We assume the amount of additional train fare only shifts commuting demands between adjacent train stations. Conventionally, the learning-and-optimization algorithm is proposed to address the bi-objective model and search the Pareto-optimal solution. In this study, we identify two major limitations of existing learning-and-optimization method and propose an improved learning-and-optimization train fare design method that uses inexact and less information to search the Pareto-optimal pricing pattern. This improvement is achieved by better utilizing the properties of the relationship between commuters' choices of their boarding/alighting train stations and train fare differences between stations. Most previous learning-and-optimization studies need accurate observation of passenger demand during the trial, while few studies notice the inaccuracy of observation and find solutions to address this issue (Han et al., 2010; Zhou et al., 2015). To the best of our knowledge, this work is the first to apply inexact information in a learning-and-optimization scheme to address a bi-objective travel demand management problem. This improvement greatly enhances the practicality of the proposed model, because the actual passenger volume is no longer needed in the train fare adjustment process. During each trial, we just need an indicator showing whether the train station is running over its capacity or not. In other words, we only need to know whether the train station is congested or not. Such an indicator can be the observed number of boarding/alighting passengers (observed demand). We already know that the observed traffic demand will be larger than the actual demand in congested scenarios. Therefore, once the observed passenger volume in a train station exceeds its designed capacity, we will know the train station is congested. We should point out that observed traffic volume is not the only practical indicator. The train dwell time is another very suitable indicator. Once the measured train dwell time is longer than the predetermined dwell time, we will know the train station is congested, otherwise, the pedestrian volume is below the train station service capacity. These indicators are very reliable criteria to measure congestion and easy to be observed in practice

which significantly strengthen the applicability of the learning-and-optimization method in the real world.

This paper is organized into six sections. Section 2 summarizes the relevant literature. In Section 3, the bi-objective optimization model is reviewed, together with the necessary assumptions and properties that would be used in this study. Section 4 presents and explains the improved learning-and-optimization scheme. Section 5 presents illustrative studies to demonstrate the efficiency of the improved learning-and-optimization method. Section 6 concludes this study.

2 Literature review

Congestion pricing is recognized as an efficient approach to deal with congestions in the transport system. The majority of existing studies about transport congestion pricing focused on the road transport networks in which the theoretical basis is the principle of marginal cost pricing (Guo and Xu, 2016; Yang and Huang, 2005). The commuters' decisions will change and move forward to the system optimum. By comparison, research on congestion pricing in rail transport systems is relatively sparse. Some aim to shift trips over time by fare adjustment. Douglas et al. (2011) modeled the fare adjustment effect on passenger flow during peak hours. Currie (2011) investigated a rail travel demand movement scheme (over time) in Melbourne. Wang et al. (2018) proposed an alternative pricing method to control the passenger demand by shifting the concentrated demand over space. A learning-and-optimization scheme was then developed that does not rely on the explicit formulation of the demand functions.

The applications of the learning-and-optimization scheme to deal with demand functions without explicit expressions/formulations have a long history. Relevant studies on the learning-and-optimization congestion pricing scheme can be classified into three categories. The first category aims to find the system optimal solution by link pricing using the learning-and-optimization method. Vickrey (1993) and Downs (1993) are the initial studies that pointed out the idea of learning-and-optimization with unknown functions. Li (2002) presented a bi-section learning-and-optimization method on a road link, which adjusts the pricing scheme

based on the relationship between observed user equilibrium traffic flow in current and previous iteration. Later, Yang et al. (2004) iteratively adjusted their pricing scheme based on the successive averages algorithm and provided its convergence proof, based on the transport network. Yang et al. (2005) presented another interesting learning-and-optimization algorithm to address the congestion-pricing problem in which the travelers' choice behavior is modeled by user equilibrium conditions; Han and Yang (2009) modeled the asymmetric and non-separable link travel impedance functions which was formulated as a variational inequality problem; Wang and Yang (2012) pointed out the convergence issue of Li (2002)'s bisection method and applied the learning-and-optimization to address it. Wang et al. (2014) extended this method to whole networks. Liu et al. (2017) proposed a practical learning-and-optimization method to address the cordon-based pricing design problem, which only needs the traffic counts.

The learning-and-optimization method is also implemented to retain link flow within a specific interval with users' value of time, link impendence functions, and travel demand functions without explicit expression. Meng et al. (2005) proposed a learning-and-optimization method to search the optimal link toll pattern with the goal of retaining the network flow within the predetermined threshold. Their method is developed from the Lagrange dual algorithm. Yang et al. (2010) further developed a PC algorithm so that the general forms of link cost functions can be applied. In addition, the algorithm achieves a faster convergence speed than Meng et al. (2005). Han et al. (2010) extended Yang et al. (2010)'s work to allow inaccurately observed traffic flow to be used in the correction stage. Meng and Liu (2011) proposed a learning-and-optimization method to address the cordon-based congestion road pricing problem. The network traffic flow is modeled by the Probit-based stochastic user equilibrium. Zhou et al. (2015) proposed a hybrid method for the learning-and-optimization method.

The third category is to integrate the learning-and-optimization method with the day-to-day dynamic network flows. This combination not only relaxes the requirement of observing equilibrium flows, but also relaxes the requirement of explicit function forms (OD demand, travel impedance), and value of time, which are hard to calibrate the accurate expressions in

practice. Ye et al. (2015) developed a learning-and-optimization algorithm to address the first-best congestion-pricing model with the excess travel cost dynamics. Guo et al. (2015) developed a dynamic road pricing model over days to manage traffic flows. Xu et al. (2016) designed a more realistic learning-and-optimization method in which the tolls can be improved at an arbitrary time interval. Zhou et al. (2019) assumed that travelers have some psychological inertia degree and proposed another learning-and-optimization pricing scheme.

This paper distinguishes itself from previous studies in two aspects. First, most of the existing learning-and-optimization methods are designed to deal with a single-objective problem. In this study, the commuting congestion alleviating problem to be addressed is bi-objective. The improved learning-and-optimization train fare design method is designed to search the corresponding Pareto-optimal pricing pattern. Second, studies mentioned above assume the traffic flows can be accurately counted/observed. This study relaxes this assumption and assumes that managers could only identify a general relationship between passenger demand and station capacity, i.e., whether the passenger volume is larger than the station capacity.

3 Problem statement

In this section, we first introduce the bi-objective optimization model and provide some necessary properties of this model. We only formulate a general relationship between the passenger flow shift and train fare increases, through some basic properties of the demand functions. Detailed discussion of this problem can refer to Wang et al. (2018). The demand functions considered in this study are deterministic, rather than stochastic (Ho and Bernal, 2019).

In this problem, four stations are considered which are denoted as S_0, S_1, S_2 and S_3. Let q_1 and q_2 denote the passenger numbers (per train) who commute at S_1 and S_2; Q denotes the capacity of a station, where $q_1 > Q$ and $q_2 > Q$; x and y denote the train fare increases of S_1 and S_2, respectively. The values of x and y are to be calculated. Note that x

and y represent the train fare difference before and after imposing train fare differentiation scheme, rather than the train fare. Let x_0 and y_0 denote the current train fares at S_1 and S_2 for a commuter before fare adjustment, the adjusted train fare equals to x_0+x and y_0+y. The spread of passenger flow depends on the fare difference between adjacent train stations. Therefore, in this study, we focus on the minimization of x and y where $x\in[0,\bar{x}]$ and $y\in[0,\bar{y}]$. The passengers of S_1 consist of three types: (i) the passengers who may shift to S_0, (ii) the passengers who always use in S_1, and (iii) the passengers who may shift to S_2. The corresponding number of passengers at S_1 are denoted as a_1, b_1, c_1, respectively. Then, the flow conservation condition holds:

$$a_1+b_1+c_1=q_1. \tag{1}$$

Let $f_1(x)$ denote the percentage of passengers in the first type who shift to S_1 and $h_1(x-y)$ denote the percentage of passengers in the third type who shift to S_1, i.e., $c_1(1-h_1(x-y))$ passengers shift to S_2. The specific expression of $f_1(x)$ and $h_1(x-y)$ is unknown. Some general assumptions of $f_1(x)$ and $h_1(x-y)$ are given:

Assumption 1: *(a)* $f_1(x)$ *and* $h_1(x-y)$ *are continuous and monotonically decreasing over* $[0,\bar{x}]$*; (b)* $f_1(0)=1$*; (c)* $0\le f_1(x)\le 1$, $x\in[0,\bar{x}]$*; (d)* $h_1(x-y)=1$, $-\bar{y}\le x-y\le 0$*; (e)* $0\le h_1(x-y)\le 1$, $0<x-y\le\bar{x}$.

The passengers at S_2 can also be categorized into three types: (i) the passengers who may shift to S_3 if y is too large, (ii) the passengers who always use S_2, (iii) the passengers who may shift to S_1 if y is higher than x. The corresponding demands of the three categories passengers are denoted as a_2, b_2, c_2, respectively. Then, the flow conservation condition holds:

$$a_2+b_2+c_2=q_2. \tag{2}$$

Let $f_2(y)$ denote the percentage of passengers in the first type who shift to S_2 and $h_2(y-x)$ denote the percentage of passengers in the third type who shift to S_2. The specific expressions of $f_2(y)$ and $h_2(y-x)$ are also absent and only some general assumptions are set:

Assumption 2*: (a)* $f_2(y)$ *and* $h_2(y-x)$ *is continuous and monotonically decreasing over* $[0,\bar{y}]$*; (b)* $f_2(0)=1$*; (c)* $0 \le f_2(y) \le 1$, $y \in [0,\bar{y}]$*; (d)* $h_2(y-x)=1$, $-\bar{x} \le y-x \le 0$*; (e)* $0 \le h_2(y-x) \le 1$, $0 < y-x \le \bar{y}$.

The number of passengers choosing S_1 and S_2 after the price increase is expressed by two functions $X(x,y)$ and $Y(x,y)$, respectively:

$$X(x,y) = a_1 f_1(x) + b_1 + c_1 h_1(x-y) + c_2(1-h_2(y-x)). \tag{3}$$

$$Y(x,y) = c_1(1-h_1(x-y)) + c_2 h_2(y-x) + b_2 + a_2 f_2(y). \tag{4}$$

For the sake of completeness, we present two properties which originally provided by Wang et al. (2018).

Property 1*: (a)* $X(x,y)$ *and* $Y(x,y)$ *are both continuous with respect to* x *and* y*; (b) given* x, $Y(x,y)$ *decreases in* y *and* $X(x,y)$ *increases in* y*; (c) given* y, $Y(x,y)$ *increases in* x *and* $X(x,y)$ *decreases in* x.

Property 2*: Increasing the same amount* $\Delta > 0$ *for* x *and* y *will not change passenger volume between* S_1 *and* S_2*, but will move passenger volume from* S_1 *to* S_0 *and from* S_2 *to* S_3*. That is,* $X(x+\Delta, y+\Delta) \le X(x,y)$ *and* $Y(x+\Delta, y+\Delta) \le Y(x,y)$.

As pointed out by Wang et al. (2018), the above formulations are very general, since the detailed function expression is absent in the real world. We only know that passengers may switch to adjacent stations with a reasonable fare increase. The objective of transport managers is to search the Pareto-optimal fare pattern so that the train fare increases at congested train stations can be minimized. Then, the mathematical model can be formulated as:

[M1] $$\min_{\substack{x\in[0,\bar{x}]\\ y\in[0,\bar{y}]}} \begin{pmatrix} x \\ y \end{pmatrix} \tag{5}$$

subject to:

$$X(x,y) \le Q \tag{6}$$

$$Y(x,y) \le Q\,. \tag{7}$$

Since [M1] is a two-objective optimization model, the solution of [M1] is Pareto-optimal. According to Theorem 1 presented in Wang et al. (2018), [M1] is equivalent to

[M2] $$\min_{\substack{x\in(0,\bar{x}]\\ y\in(0,\bar{y}]}} \begin{pmatrix} x \\ y \end{pmatrix} \tag{8}$$

subject to:

$$X(x,y) = Q \tag{9}$$

$$Y(x,y) = Q\,. \tag{10}$$

Intuitively, the Pareto-optimal solution is a space among the domain. However, according to Theorem 3 in Wang et al. (2018), [M2] has a unique solution, which implies [M1] also has a unique solution. Therefore, solving [M1] just needs to find out the unique feasible solution, which is discussed in detail in the next section.

4 An improved learning-and-optimization scheme with unknown demand functions

A learning-and-optimization method (algorithm 1) was proposed by Wang et al. (2018). The basic idea of this method is to make a trial to obtain more information and eliminate the infeasible regions based on the learned information. As shown in Table 1, for any trial of $\left(x^{(n)}, y^{(n)}\right)$ at iteration n, there are six scenarios. Each scenario matches a specific infeasible domain which should be eliminated. As shown in Table 1, the remaining feasible domain is still a rectangle and the feasible regions could be iteratively restricted until the solution is found.

Table 1 Identification of infeasible regions at iteration n.

(i) $X^{(n)} \geq Q,\ Y^{(n)} \geq Q,\ X^{(n)} + Y^{(n)} > 2Q.$

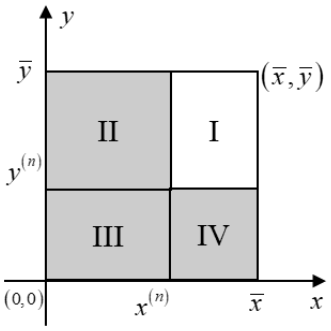

(ii) $X^{(n)} \leq Q,\ Y^{(n)} \leq Q,\ X^{(n)} + Y^{(n)} < 2Q.$

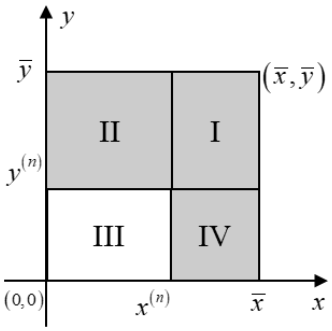

(iii) $X^{(n)} \geq Q,\ Y^{(n)} \leq Q,\ X^{(n)} + Y^{(n)} \geq 2Q.$

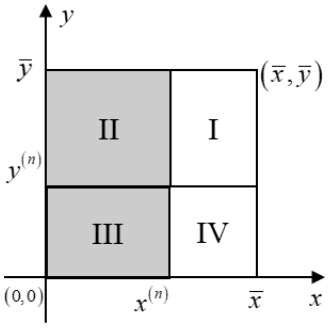

(iv) $X^{(n)} \geq Q,\ Y^{(n)} \leq Q,\ X^{(n)} + Y^{(n)} \leq 2Q.$

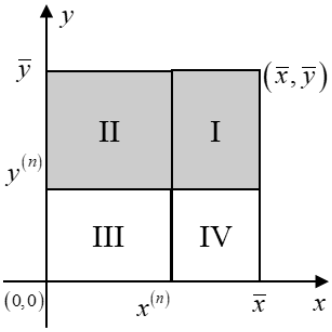

(v) $X^{(n)} \leq Q,\ Y^{(n)} \geq Q,\ X^{(n)} + Y^{(n)} \geq 2Q.$

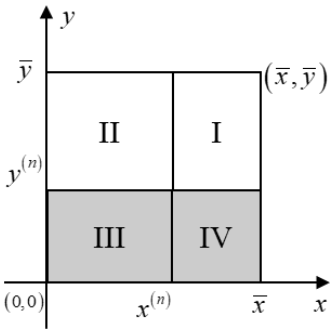

(vi) $X^{(n)} \leq Q,\ Y^{(n)} \geq Q,\ X^{(n)} + Y^{(n)} \leq 2Q.$

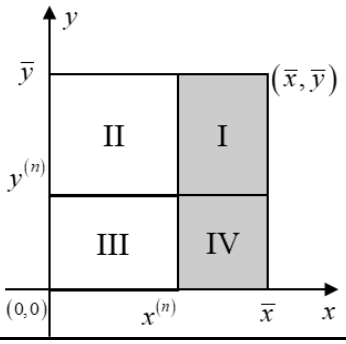

Although the proposed method could converge, this method has two major limitations: (a) it needs to calculate the total demand of both S_1 and S_2, i.e., $X^{(n)} + Y^{(n)}$, to identify infeasible regions, however, this value cannot be precisely obtained in practice; (b) it did not fully utilize the properties of the proposed model. On the one hand, if the observed X or Y is larger than Q, this means the commuting congestion has happened. The trains including the following trains will be delayed and stay in upstream stations. It would allow more passengers to get on/off the trains at upstream stations and then, result in a biased observation of X or Y. Therefore, it is hard to precisely observe $X^{(n)}$ or $Y^{(n)}$ during peak hours. On the other hand, the rules defined in Table 1, i.e., case (iii)–case (vi), are mainly based on the monotonicity

stated by Property 1 (Detailed descriptions can be found in Wang et al. (2018)). However, Property 2 provides us more information to identify more infeasible regions, which are not considered in Table 1. In this study, we show that without the exact demand of $X^{(n)}+Y^{(n)}$, we could still efficiently identify the infeasible regions and find the Pareto-optimal price scheme. In this regard, case (iii) and case (iv) in Table 1 are combined as one case (denoted as case (a)), and the case (v) and case (vi) in Table 1 are combined as another case (denoted as case (b)). Then, we have the following properties:

Property 3: *Given the case (a), i.e.,* $X^{(n)} \geq Q$, $Y^{(n)} \leq Q$. *Suppose* $\left(x^{(n)}, y^{(n)}\right)$ *is the new trial point, the infeasible regions for this case could be formed by the line* $l:\ y = x + \left(y^{(n)} - x^{(n)}\right)$. *All the points in the black region (on and above the line* l*) as shown in Figure 2 are infeasible.*

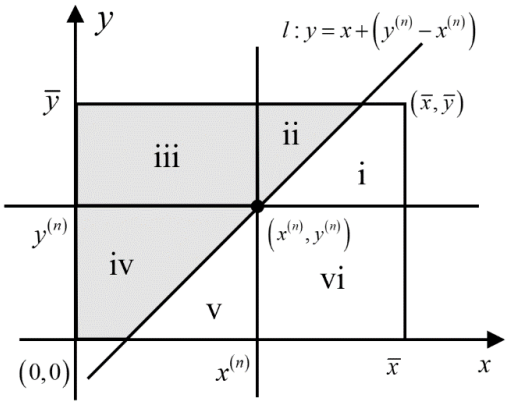

Figure 2 Infeasible regions for case: $X^{(n)} \geq Q$, $Y^{(n)} \leq Q$.

Proof: Consider the case of adjusting (x, y) along the line $l:\ y = x + \left(y^{(n)} - x^{(n)}\right)$, i.e., adjust (x, y) with the same amount of price Δ. According to Property 2, it is easy to see that: (i) if $\Delta > 0$, then $Y(x+\Delta, y+\Delta) \leq Y(x, y)$ and $X(x+\Delta, y+\Delta) \leq X(x, y)$ where $x+\Delta \in [0, \bar{x}]$ and $y+\Delta \in [0, \bar{y}]$; (ii) if $\Delta < 0$, then $Y(x+\Delta, y+\Delta) \geq Y(x, y)$ and $X(x+\Delta, y+\Delta) \geq X(x, y)$ where $x+\Delta \in [0, \bar{x}]$ and $y+\Delta \in [0, \bar{y}]$. That means the points on the line l cannot lead X and

Y converge on Q simultaneously. Therefore, the points on the line l can be identified as infeasible.

Then, we consider the points above the line l which can be classified into three cases. (i) If the point is within region ii, this point can be represented as $(x+\Delta, y+\Delta+\Delta')$ where $\Delta>0$ and $\Delta'>0$. According to Property 1, $Y(x,y)$ is monotonically decreasing in y, therefore, $Y(x+\Delta, y+\Delta+\Delta') \le Y(x+\Delta, y+\Delta) \le Y(x,y) \le Q$. That is, the points within region ii lead to Y further smaller than Q. Therefore, region ii is infeasible. (ii) If the point is within region iv, this point can be represented as $(x+\Delta, y+\Delta+\Delta')$ where $\Delta<0$ and $\Delta'>0$. As $\Delta<0$, we have $X(x+\Delta, y+\Delta) \ge X(x,y)$. In addition, according to Property 1, $X(x,y)$ is monotonically increasing in y, thus, we have $X(x+\Delta, y+\Delta+\Delta') \ge X(x+\Delta, y+\Delta)$ and $X(x+\Delta, y+\Delta) \ge X(x,y) \ge Q$. In other words, the points in region iv cannot lead X converge to Q. Therefore, region iv is infeasible. (iii) If the point is within region iii, this point can be represented as $(x-\Delta', y+\Delta'')$ where $\Delta'>0$, $\Delta''>0$, $x-\Delta' \ge 0$, and $y+\Delta'' \le \bar{y}$. According to Property 1, it is easy to see $X(x,y)$ is monotonically increasing in y and monotonically decreasing in x, and $Y(x,y)$ is monotonically increasing in x and monotonically decreasing in y. Then, we have $Q \le X(x,y) \le X(x-\Delta', y+\Delta'')$ and $Q \ge Y(x,y) \ge Y(x-\Delta', y+\Delta'')$, and region iii is infeasible.

□

Property 4: *Given the case (b), i.e.,* $X^{(n)} \le Q$, $Y^{(n)} \ge Q$. *Suppose* $(x^{(n)}, y^{(n)})$ *is the new trial point, the infeasible regions for this case could be formed by the line* $l:\ y = x + (y^{(n)} - x^{(n)})$. *All the points in the black triangle region (on and below the line* l*) as shown in Figure 3 are infeasible.*

Proof: We first consider the case of adjusting (x,y) along the line $l:\ y = x + (y^{(n)} - x^{(n)})$, i.e., adjust (x,y) with the same amount of price Δ. According to Property 2, it is easy to see that:

(i) if $\Delta > 0$, then $X(x+\Delta, y+\Delta) \le X(x, y)$ and $Y(x+\Delta, y+\Delta) \le Y(x, y)$ where $x+\Delta \le \bar{x}$ and $y+\Delta \le \bar{y}$; (ii) if $\Delta < 0$, then $X(x+\Delta, y+\Delta) \ge X(x, y)$ and $Y(x+\Delta, y+\Delta) \ge Y(x, y)$ where $0 \le x+\Delta$ and $0 \le y+\Delta$. That means the points on the line l cannot lead X and Y converge to Q simultaneously. Therefore, the points on the line l can be identified as infeasible.

The points below the line l can be classified into three regions, i.e., region i, v and vi. (i) If the point is within region i, this point can be represented as $(x+\Delta, y+\Delta-\Delta')$ where $\Delta > 0$ and $\Delta' > 0$. According to Property 1, $X(x, y)$ is monotonically increasing in y, therefore, $X(x+\Delta, y+\Delta-\Delta') \le X(x+\Delta, y+\Delta) \le X(x, y) \le Q$. In other words, the points within region i lead to X further smaller than Q. Therefore, region i is infeasible. (ii) If the point is within region v, this point can be represented as $(x+\Delta, y+\Delta+\Delta')$ where $\Delta < 0$ and $\Delta' < 0$. As $\Delta < 0$, we have $Y(x+\Delta, y+\Delta) \ge Y(x, y)$. In addition, according to Property 1, $Y(x, y)$ is monotonically decreasing in y, thus, we have $Y(x+\Delta, y+\Delta+\Delta') \ge Y(x+\Delta, y+\Delta)$ and $Y(x+\Delta, y+\Delta) \ge Y(x, y) \ge Q$. In other words, the points in region v cannot lead Y converge to Q. Therefore, region v is infeasible. (iii) If the point is within region vi, this point can be represented as $(x+\Delta, y-\Delta)$ where $\Delta > 0$. According to Property 1, it is easy to see $X(x, y)$ is monotonically increasing in y and monotonically decreasing in x, and $Y(x, y)$ is monotonically increasing in x and monotonically decreasing in y. Then, we have $Q \ge X(x, y) \ge X(x+\Delta, y-\Delta)$ and $Q \le Y(x, y) \le Y(x+\Delta, y-\Delta)$, and region vi is infeasible.

□

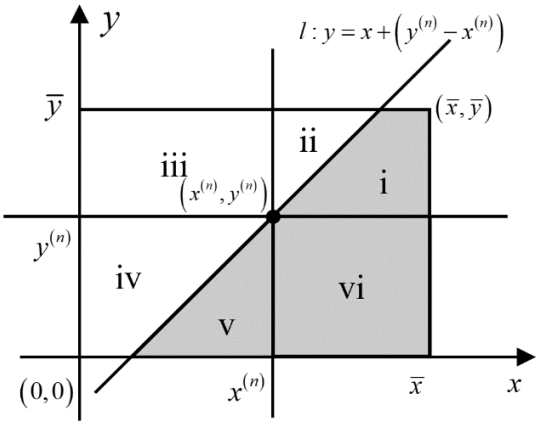

Figure 3 The infeasible regions for case: $X^{(n)} \le Q$, $Y^{(n)} \ge Q$.

The idea becomes clear. Based on Property 3 and Property 4, we only need to know whether the train station is congested, i.e., $X^{(n)} \ge Q$, and $Y^{(n)} \ge Q$. Although the observed $\tilde{X}^{(n)}$ and $\tilde{Y}^{(n)}$ are inexact, we can still infer the congestion status. In the scenarios that one station is congested and another is free, we could identify infeasible regions without requiring the observation of total demand $X^{(n)} + Y^{(n)}$, by using Property 3 and 4. In scenarios that both stations are congested or free, we can identify infeasible regions based on Property 1. In this way, Table 1 could be refined from six scenarios to four scenarios. Table 2 shows the refined infeasible regions that can be identified by inexact and less information. Note that the domains could be irregular in the calculation, as shown in Appendix A. For simplicity, Table 2 uses the rectangle domain to illustrate the idea. Therefore, the infeasible region elimination procedure could be summarized as follows.

Suppose at step n, an arbitrary trial of fare increases $\left(x^{(n)}, y^{(n)}\right)$ is implemented to make commuting passengers shift their boarding/alighting train stations. The changed demands of passengers are then observed, i.e., $\tilde{X}^{(n)}$ and $\tilde{Y}^{(n)}$. The observed information could identify the infeasible region since the certain region of the domain D cannot lead to a feasible solution, despite the specific observation of demand is inexact. By comparing the observed $\tilde{X}^{(n)}$, $\tilde{Y}^{(n)}$ with Q, one of the four scenarios presented in Table 2 will be matched. For example, in case (a) of Table 2, the observed passenger volumes show that $\tilde{X}^{(n)} \ge Q$, $\tilde{Y}^{(n)} \le Q$, and then the

next trial $\left(x^{(n+1)}, y^{(n+1)}\right)$ should be taken within a restricted area indicated by region i, v, and vi, while infeasible regions ii, iii, and iv should be eliminated. In region i, increasing both x and y ($x \geq y$) leads to $X^{(n+1)} \leq X^{(n)}$, adding with the learned information $\tilde{X}^{(n)} \geq Q$, then $X^{(n+1)}$ may converge to Q. In region vi, increasing x and decreasing y leads to $X^{(n+1)} \leq X^{(n)}$ and $Y^{(n+1)} \geq Y^{(n)}$, adding with the previously observed result $\tilde{X}^{(n)} \geq Q$ and $\tilde{Y}^{(n)} \leq Q$, then $X^{(n+1)}$ and $Y^{(n+1)}$ may converge to Q. The same reason is for region v which indicates $Y^{(n+1)} \geq Y^{(n)}$.

Table 2 infeasible regions of the domain (improved method).

(a) $\tilde{X}^{(n)} \geq Q$, $\tilde{Y}^{(n)} \leq Q$.

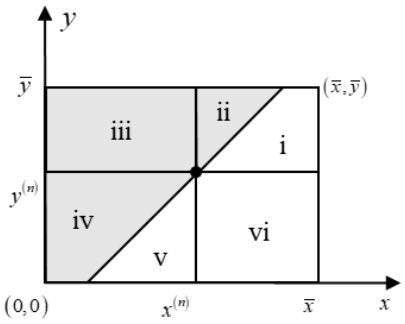

(b) $\tilde{X}^{(n)} \leq Q$, $\tilde{Y}^{(n)} \geq Q$.

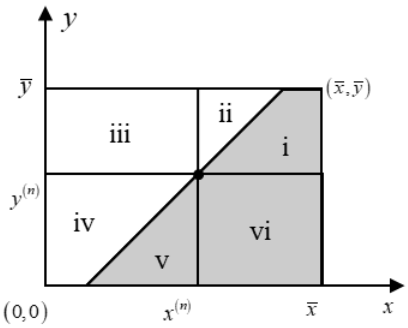

(c) $\tilde{X}^{(n)} \geq Q$, $\tilde{Y}^{(n)} \geq Q$.

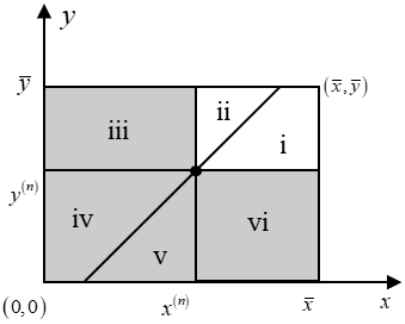

(d) $\tilde{X}^{(n)} \leq Q$, $\tilde{Y}^{(n)} \leq Q$.

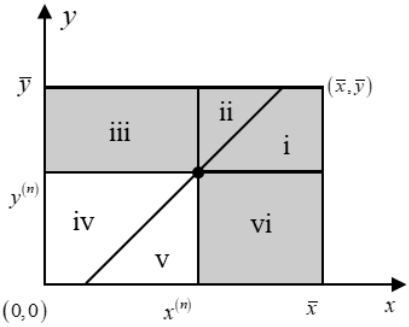

Note that the restricted area formed by Table 2 is still convex. The regions that could be generated based on Table 2 are shown in Appendix A.

Definition 1: *Let V denote a real vector space. Given two points $\mu, v \in V$, all convex combinations of μ and v can be expressed as*

$$\left\{w_\lambda \in V : w_\lambda = (1-\lambda)\mu + \lambda v, 0 \leq \lambda \leq 1\right\}. \tag{11}$$

Definition 2: *Let* $K \subset V$ *. If any two points* $\mu, v \in K$ *, the set of all convex combinations of* μ *and* v *is a subset of* K *, then set* K *is convex.*

Definition 1 defines convex combinations and Definition 2 defines convex set which means a set is convex if it contains all convex combinations of any pair of its points (Boyd and Vandenberghe, 2004).

Proposition 1: *The reduced/restricted region formed by Table 2 is always a convex polygon.*

With the assist of Proposition 1, the convexity can always hold during the feasible region restriction process. The proof is given in Appendix B. Note that an arbitrary trial of fare increases (x, y) could eliminate a part of infeasible regions. However, it cannot ensure its convergence rate. It is important to find a fast/efficient way to find the Pareto-optimal prices. Thus, a trial point definition/selection method could be proposed to ensure its fast convergence rate. Denote the area of a region as A, e.g., A_I denotes the area of region i, then, the trial point should subject to the following two equations:

$$A_I + A_V + A_{VI} = A_{II} + A_{III} + A_{IV} \tag{12}$$

$$A_I + A_{II} = A_{IV} + A_V \tag{13}$$

where Eq. (12) means the area of the region formed by region i, v, and vi and the area of the region formed by region ii, iii, and iv are the same, which means either case (a) or case (b) happens, definitely half of the testing region can be identified as infeasible. Eq. (13) means the area of the region formed by region i, and ii and the area of the region formed by region iv, and v are the same, which means more than half of the testing region can be identified as infeasible, no matter case (c) or case (d) happens. Therefore, Eq. (12) and Eq. (13) ensure at least half of the domain in the previous iteration could be identified as infeasible in each iteration. In other

words, the price adjustment scheme would converge to its optimal solution at the exponential convergence rate. We have:

Proposition 2: *Given an error* $\varepsilon > 0$*, the Pareto-optimal prices can be found in time at most* $\lceil \log_2 \overline{x} \cdot \overline{y} / \varepsilon \rceil$ *by using the proposed trial point update method, i.e., Eq. (12)–Eq. (13).*

Proof: Given $\overline{x}$ and $\overline{y}$, the initial area formed by $\overline{x}$ and $\overline{y}$ is denoted as $\overline{x} \cdot \overline{y}$. We find the Pareto-optimal prices by bi-section section search. Following Eq. (12) and Eq. (13), we have: (1) If case (a) or (b) happens, 50 percent of the region can be eliminated; (2) If case (c) or (d) happens, more than 50 percent of the region can be eliminated; Even consider the worst case, i.e., always 50 percentage area is eliminated at each iteration, the testing region can still shrink at the exponential rate. Let t denote the times that the trial needs to find the Pareto-optimal prices, we have $2^t = \overline{x} \cdot \overline{y} / \varepsilon$. In other words, if the Pareto-optimal prices have not been found, we proceed to identify and eliminate the infeasible regions, which can be done in time at most $\lceil \log_2 \overline{x} \cdot \overline{y} / \varepsilon \rceil$.

□

Note that solving Eq. (12) and Eq. (13) may be a bit tedious, as the updated domain is sometimes irregular (despite convex). In this regard, we propose an alternative method to update the trial point. We use centroid to approximate the condition Eq. (12)–(13) which can be written as (Bourke, 1988):

$$x^{(n+1)} = \frac{1}{6A} \sum_{i=0}^{m-1} \left(x_i + x_{i+1} \right) \left(x_i y_{i+1} - x_{i+1} y_i \right), \tag{14}$$

$$y^{(n+1)} = \frac{1}{6A} \sum_{i=0}^{m-1} \left(y_i + y_{i+1} \right) \left(x_i y_{i+1} - x_{i+1} y_i \right), \tag{15}$$

where (x_i, y_i) are the vertices of the polygon and m is the number of vertices; A is the polygon's signed area, as described by the shoelace formula:

$$A = \frac{1}{2}\sum_{i=1}^{m-1}\left(x_i y_{i+1} - x_{i+1} y_i\right). \tag{16}$$

In these formulae, the vertices are indexed in order of their occurrence along the polygon's perimeter and the last vertex (x_m, y_m) is defined to be the same as the first vertex (x_0, y_0). Based on the above analyses, an improved learning-and-optimization algorithm (algorithm 2) is presented as follows.

Algorithm 2. *An improved learning-and-optimization algorithm.*

Step 0: Let $n = 0$; error gap $\varepsilon_1 > 0$; $(x, y) \in D^{(0)} := [0, \bar{x}] \times [0, \bar{y}]$.

Step 1: Update the fare increase $\left(x^{(n+1)}, y^{(n+1)}\right)$ by solving the Eq. (12) and Eq. (13) or Eq. (14) and Eq. (15).

Step 2: Observe $\tilde{X}^{(n+1)}$ and $\tilde{Y}^{(n+1)}$. If $Q - \varepsilon_1 \le \tilde{X}^{(n+1)} \le Q + \varepsilon_1$ and $Q - \varepsilon_1 \le \tilde{Y}^{(n+1)} \le Q + \varepsilon_1$, $\left(x^{(n+1)}, y^{(n+1)}\right)$ is the Pareto-optimal solution and terminate.

Step 3: Eliminate the infeasible domain according to Table 2 and update the domain $D^{(n+1)}$, which is at most half the size of $D^{(n)}$. Let $n = n + 1$ and go back to Step 1.

Considering the real situation in which the unit of train fare is usually set as 1 cent, the train fare should only be an integer multiple of cents. Therefore, we further revise algorithm 2 and present a slightly modified algorithm (algorithm 3). For algorithm 3, we have the following property:

Proposition 3: *An ε-optimal solution can be found at most* $\lceil \log_2 \bar{x} \rceil + \lceil \log_2 \bar{y} \rceil$ *iterations in the worst case.*

Considering the case that $\bar{x}$ and $\bar{y}$ is one thousand cents, according to Proposition 3, we only need 20 iterations to obtain the Pareto-optimal solution even in the worst case. The details of algorithm 3 are presented as follows.

Algorithm 3. *An improved learning-and-optimization algorithm.*

Step 0: Let $n=0$; $(x,y)\in D^{(0)}:=[0,\bar{x}]\times[0,\bar{y}]$; error gap $\varepsilon_1>0$.

Step 1: Update the fare increase $\left(x^{(n+1)},y^{(n+1)}\right)$ by solving the Eq. (12) and Eq. (13) or Eq. (14) and Eq. (15).

Let $\left(x^{(n+1)},y^{(n+1)}\right)\leftarrow\left(\left\lfloor x^{(n+1)}\right\rfloor,\left\lfloor y^{(n+1)}\right\rfloor\right)$ where $\lfloor\cdot\rfloor$ denotes the floor function.

Step 2: Observe $\tilde{X}^{(n+1)}$ and $\tilde{Y}^{(n+1)}$. If $Q-\varepsilon_1\le\tilde{X}^{(n+1)}\le Q+\varepsilon_1$ and $Q-\varepsilon_1\le\tilde{Y}^{(n+1)}\le Q+\varepsilon_1$, $\left(x^{(n+1)},y^{(n+1)}\right)$ is an approximated Pareto-optimal solution.

Step 3: We consider the following four cases:

Case 3.1:	$\bar{x}^{(n)}-\underline{x}^{(n)}=1,\ \bar{y}^{(n)}-\underline{y}^{(n)}=1$	$\left(x^{(n+1)},y^{(n+1)}\right)$ is an approximated Pareto-optimal solution.
Case 3.2:	$\bar{x}^{(n)}-\underline{x}^{(n)}=1,\ \bar{y}^{(n)}-\underline{y}^{(n)}>1$	If $\tilde{Y}^{(n+1)}>Q$, adjust the domain by updating $\underline{y}=y^{(n+1)}$. If $\tilde{Y}^{(n+1)}<Q$, adjust the domain by updating $\bar{y}=y^{(n+1)}$. Set $n=n+1$ and go back to Step 1.
Case 3.3:	$\bar{x}^{(n)}-\underline{x}^{(n)}>1,\ \bar{y}^{(n)}-\underline{y}^{(n)}=1$	If $\tilde{X}^{(n+1)}>Q$, adjust the domain by updating $\underline{x}=x^{(n+1)}$. If $\tilde{X}^{(n+1)}<Q$, adjust the domain by updating $\bar{x}=x^{(n+1)}$. Set $n=n+1$ and go back to Step 1.
Case 3.4:	$\bar{x}^{(n)}-\underline{x}^{(n)}>1,\ \bar{y}^{(n)}-\underline{y}^{(n)}>1$	Eliminate the infeasible domain according to Table 2. Set n=n+1 and go back to Step 1.

5 Numerical experiments

We consider each train has eight carriages and each carriage has three doors and suppose each door can let approximately two passengers get on/off the carriage per second and the designed dwelling time is 15 seconds at each train station along the rail line. Then, the designed

boarding/alighting ability Q should be 720 ($15\times8\times3\times2$) passengers per train. If the actual commuting demand is larger than the planned threshold value, the dwell time will also be longer than the preplanned time interval and will rely on the commuting passenger volume. We assume neighboring stations of S_1 and S_2 are uncongested and the dwell times are still equal to 15 seconds, while dwelling times of the S_1 and S_2 are larger than 15 seconds due to the excess commuting demands (q_1 and q_2). Here, we suppose $q_1 = 800$ which consists of three categories $a_1 = 200$, $b_1 = 400$, $c_1 = 200$. Similarly, we assume $q_2 = 850$ at S_2, with $a_2 = 200$, $b_2 = 400$, $c_2 = 250$. The numerical settings are hypothetically created to obtain some insights.

Table 3 Unknown demand functions.

Passenger demand functions:
$f_1(x) = \exp(-x)$, $0 \le f_1(x) \le 1, x \in [0, \bar{x}]$.
$h_1(x-y) = \begin{cases} 1, & -\bar{y} \le x-y \le 0 \\ 1-(x-y)^2/\bar{x}^2, & 0 < x-y \le \bar{x}. \end{cases}$
$f_2(x) = \exp(-0.5x)$, $0 \le f_2(x) \le 1, x \in [0, \bar{x}]$.
$h_2(y-x) = \begin{cases} 1, & -\bar{x} \le y-x \le 0 \\ 1-(y-x)^2/(2\bar{y}^2), & 0 < y-x \le \bar{y}. \end{cases}$

The additional price is imposed on the two congested CBD train stations S_1 and S_2 to reduce the commuting demands q_1 and q_2. If the commuting demands are well managed to be no larger than Q, the trains' dwell time will return to 15 seconds during peak hours. The functions in Table 3 simulate the passengers' actual response (actual demand). $\bar{x}$ and $\bar{y}$ are set to be 5 and 3 dollars, respectively. Recall that the improved learning-and-optimization method only needs to identify whether the boarding/alighting demands exceed the corresponding capacity. The demands calculated by the functions assumed in Table 3 are actual demands, and the observed demands will be larger than the actual demands in congestion

scenarios. When congestion happens, the number of observed boarding/alighting passengers (observed demand) depends on many influence factors and specific situations which are hard to predict. Therefore, in the illustrative examples, we set the observed demand to be a random variable. Specifically, when the actual demand X (or Y) exceeds 101% of Q, the corresponding observed demand $\tilde{X}$ (or $\tilde{Y}$) is generated from the uniform distribution $U[X,1.5X]$ (or $U[Y,1.5Y]$).

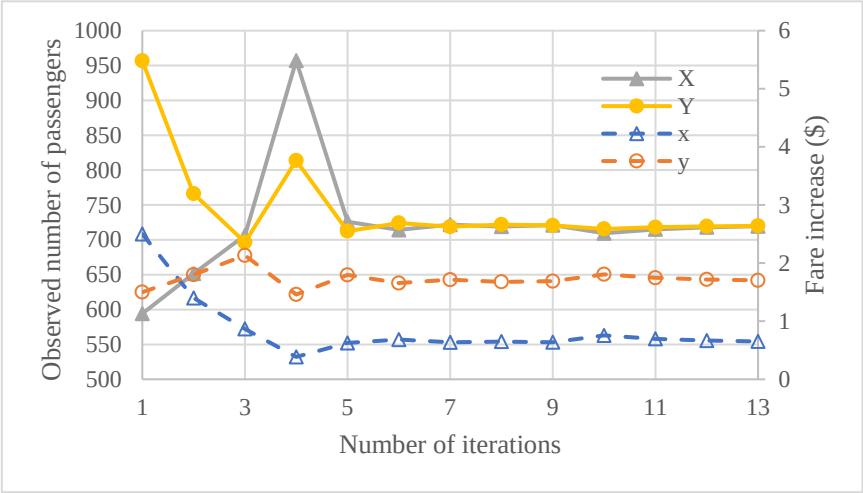

(a) The convergence of algorithm 2.

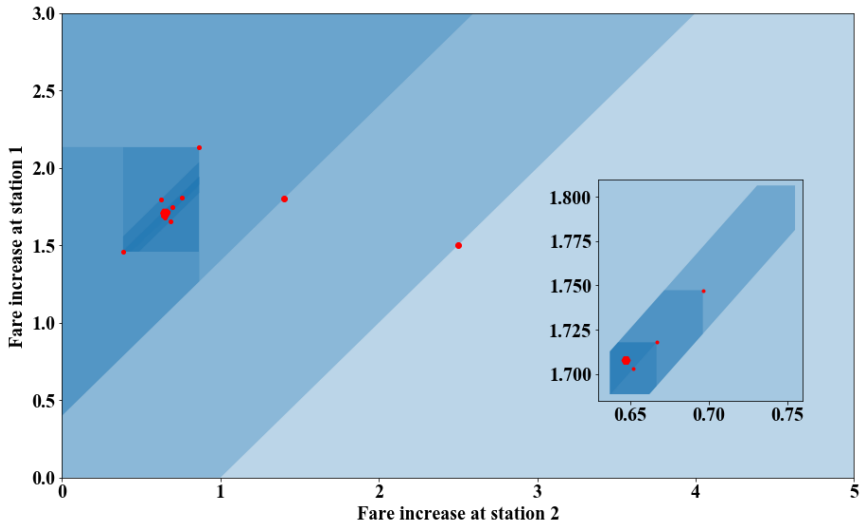

(b) The shrink progress of the fare increases domain.

Figure 4 The convergence of algorithm 2.

Then, we use algorithm 2 to address this problem. The error gap is set at ε=1. In other words, given a price scheme (x^*, y^*), if the corresponding controlled boarding/aligning

passengers are within the ranges $Q-\varepsilon \le \tilde{X} \le Q+\varepsilon$ and $Q-\varepsilon \le \tilde{Y} \le Q+\varepsilon$, we can conclude that the algorithm has obtained the Pareto-optimal pricing solutions (x^*, y^*). The detailed calculation steps are shown in Figure 4 and Table 4.

Table 4 Calculation procedure of algorithm 2.

n	x	y	$\tilde{X}$	$\tilde{Y}$	$\underline{x}$	$\overline{x}$	$\underline{y}$	$\overline{y}$	$\underline{l}$	$\overline{l}$	Case
1	2.500	1.500	594.194	956.802	0.000	5.000	0.000	3.000	(2.500, 1.500)	–	(ii)
2	1.400	1.800	651.541	766.184	0.000	5.000	0.000	3.000	(1.400, 1.800)	–	(ii)
3	0.866	2.133	706.354	696.546	0.000	0.866	0.000	2.133	(1.400, 1.800)	–	(iv)
4	0.385	1.459	957.018	813.773	0.385	0.866	1.459	2.133	(1.400, 1.800)	–	(iii)
5	0.625	1.796	725.977	712.440	0.385	0.866	1.459	2.133	(1.400, 1.800)	(0.625,1.796)	(i)
6	0.683	1.656	714.149	724.211	0.385	0.866	1.459	2.133	(0.683, 1.656)	(0.625,1.796)	(ii)
7	0.637	1.713	721.770	718.800	0.385	0.866	1.459	2.133	(0.637, 1.713)	(0.625,1.796)	(i)
8	0.649	1.676	719.060	721.878	0.385	0.866	1.459	2.133	(0.637, 1.713)	(0.649,1.676)	(ii)
9	0.637	1.688	721.094	720.618	0.637	0.866	1.688	2.133	(0.637, 1.713)	(0.649,1.676)	(iii)
10	0.755	1.806	709.352	715.702	0.637	0.755	1.688	1.806	(0.637, 1.713)	(0.649,1.676)	(iv)
11	0.696	1.747	715.019	718.144	0.637	0.696	1.688	1.747	(0.637, 1.713)	(0.649,1.676)	(iv)
12	0.666	1.717	717.997	719.381	0.637	0.666	1.688	1.717	(0.637, 1.713)	(0.649,1.676)	(iv)
13	0.652	1.703	**719.529**	**720.001**	0.637	0.666	1.688	1.717	(0.652, 1.703)	(0.649,1.676)	(ii)

In Figure 4 (a), the evaluation process of fare increases of the station S_1 and S_2 are shown by dash lines x and y. The corresponding observed commuting volumes of the station S_1 and S_2 are shown by lines X and Y. We note that the observed X, Y are random in congestion scenarios. Figure 4 (a) shows that both X and Y rapidly approximate the target volume Q with 13 iterations. In the 13th iteration, the adjusted X and Y are 719.529 and 720.001. The fare increases are 0.652148 and 1.70323, respectively, which are the Pareto-optimal solutions. Figure 4 (b) shows the shrink progress of the fare increases domain. The red points reflect the trial point which is located at the geometric center of the domain. In each trial, approximately half of the domain is eliminated, and the domain is iteratively contracted until the termination criterion is reached.

Table 4 presents more details of the improved algorithm. Columns x, y, $\tilde{X}$, $\tilde{Y}$ in Table 4 correspond to the lines x, y, X, Y in Figure 4(a). The following columns $\underline{x}$, $\overline{x}$, $\underline{y}$, $\overline{y}$, $\underline{l}$, and $\overline{l}$ in Table 4 represent the boundaries of x and y, respectively.

Compared to algorithm 1 proposed by Wang et al. (2018), additional boundaries, $\underline{l}$ and $\overline{l}$, are attached, therefore, more properties of the problem [M2] are utilized. In each iteration, a certain region of the domain formed by $\underline{x}$, $\overline{x}$, $\underline{y}$, $\overline{y}$, $\underline{l}$, and $\overline{l}$ can be identified as infeasible, according to the observation of corresponding commuting volumn $\tilde{X}$ and $\tilde{Y}$. The region elimination pattern is reported in the last column of Table 4. The feasible regions formed by these boundaries as shown in Figure 4 (b) are iteratively smaller, which indicates the convergence efficiency.

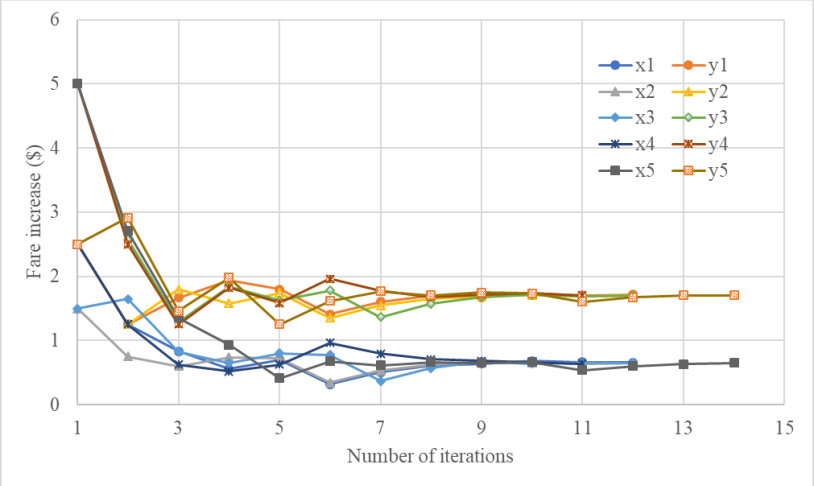

(a) The convergence of train fare increases

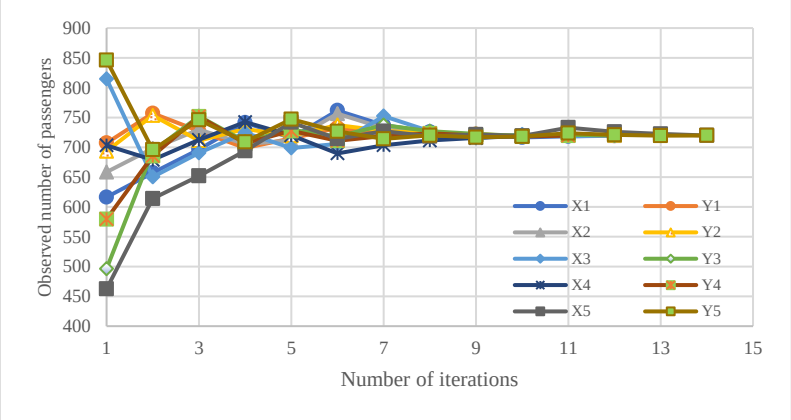

(b) The convergence of the number of passengers

Figure 5 The convergence of algorithm 2 with various initial points.

To further validate the proposed algorithm, we conduct a series of tests with respect to various initial train fare increases settings, $\left(x^{(0)}, y^{(0)}\right)$. Specifically, five different initial fare increases settings are tested: (3, 5), (3, 10), (5, 5), (5, 10) and (10, 5). Figure 5 shows the

evaluation process of passenger boarding/alighting demand and the fare charge pattern. Results indicate that algorithm 2 converges rapidly no matter what the initial state is.

We further compare algorithms 1 and 2 regarding their converge trend and details of results in Figure 6 and Table 5, respectively. Generally, algorithms 1 and 2 show a similar convergence trend. Although algorithm 1 reaches the accuracy criterion at the 11^{th} iteration, the absolute error is still weaker than algorithm 2. Both of them iterate 13 times to achieve almost the same precision level. This phenomenon demonstrates that algorithm 2 has the same convergence rate as algorithm 1. Note that algorithm 2 utilizes Property 3 and Property 4 to identify the infeasible regions, while algorithm 1 utilizes the relationship between $X+Y$ and $2Q$ to identify the infeasible regions.

To align with the real situation, we set the unit of price as 0.01 dollars and apply algorithm 3 to search the Pareto-optimal pricing scheme. Figure 7 shows the convergence trend, which reached predetermined accuracy criteria at the 12th iteration. Details of the calculation process are shown in Table 6.

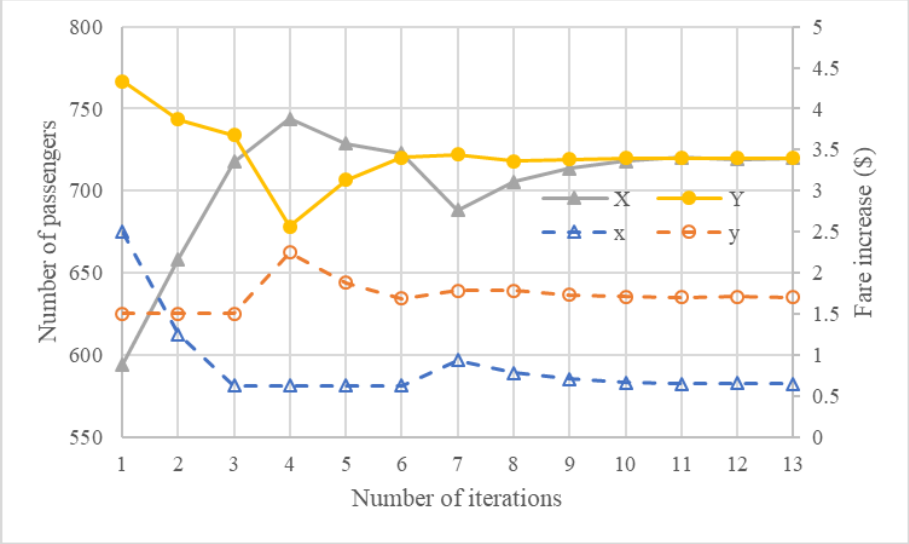

Figure 6 The evaluation process of algorithm 1.

Table 5 Calculation procedure of algorithm 1.

n	x	y	$\tilde{X}$	$\tilde{Y}$	$\underline{x}$	$\bar{x}$	$\underline{y}$	$\bar{y}$	Case
1	2.5	1.5	594.194	766.695	0	2.5	0	3	(vi)
2	1.25	1.5	658.169	743.605	0	1.25	0	3	(vi)
3	0.625	1.5	717.685	733.839	0	1.25	1.5	3	(v)
4	0.625	2.25	743.727	678.255	0	1.25	1.5	2.25	(iv)
5	0.625	1.875	728.753	706.619	0	1.25	1.5	1.875	(iv)
6	0.625	1.687	722.731	720.339	0.625	1.25	1.687	1.875	(i)
7	0.937	1.781	688.208	722.192	0.625	0.937	1.687	1.875	(vi)

8	0.781	1.781	705.455	718.191	0.625	0.781	1.687	1.781	(ii)
9	0.703	1.734	713.777	719.255	0.625	0.703	1.687	1.734	(ii)
10	0.664	1.71	718.172	719.795	0.625	0.664	1.687	1.71	(ii)
11	0.644	1.699	720.431	720.066	0.644	0.664	1.699	1.71	(i)
12	0.654	1.705	719.296	719.93	0.644	0.654	1.699	1.705	(ii)

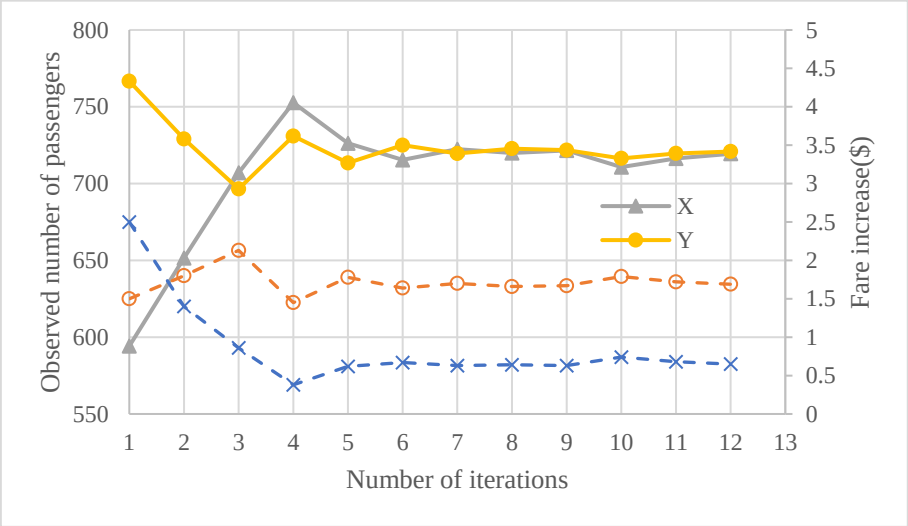

Figure 7 The evaluation process of algorithm 3.

Table 6 Calculation procedure of algorithm 3.

n	x	y	$\tilde{X}$	$\tilde{Y}$	$\underline{x}$	$\overline{x}$	$\underline{y}$	$\overline{y}$	$\underline{l}$	$\overline{l}$	Case
1	2.50	1.50	594.194	768.435	0.00	5.00	0.00	3.00	(2.50, 1.50)	-	(ii)
2	1.40	1.80	651.541	730.091	0.00	5.00	0.00	3.00	(1.40, 1.80)	-	(ii)
3	0.86	2.13	707.033	696.544	0.00	0.86	0.00	2.13	(1.40, 1.80)	-	(iv)
4	0.38	1.45	755.673	730.963	0.38	0.86	1.45	2.13	(1.40, 1.80)	-	(iii)
5	0.62	1.78	726.277	713.442	0.38	0.86	1.45	2.13	(1.40, 1.80)	(0.62, 1.78)	(i)
6	0.67	1.64	715.409	725.018	0.38	0.86	1.45	2.13	(0.67, 1.64)	(0.62, 1.78)	(ii)
7	0.63	1.70	722.419	719.581	0.38	0.86	1.45	2.13	(0.67, 1.64)	(0.63, 1.70)	(i)
8	0.64	1.66	719.908	722.759	0.38	0.86	1.45	2.13	(0.64, 1.66)	(0.63, 1.70)	(ii)
9	0.63	1.67	721.540	721.752	0.63	0.86	1.67	2.13	(0.64, 1.66)	(0.63, 1.70)	(iii)
10	0.74	1.79	710.735	716.409	0.63	0.74	1.67	1.79	(0.64, 1.66)	(0.63, 1.70)	(iv)
11	0.68	1.72	716.345	719.610	0.63	0.68	1.67	1.72	(0.64, 1.66)	(0.63, 1.70)	(iv)
12	0.65	1.69	**719.431**	**720.889**	0.63	0.68	1.67	1.72	(0.65, 1.69)	(0.63, 1.70)	(ii)

6 Conclusions

This study proposed an improved learning-and-optimization algorithm to search the Pareto-optimal train fare pattern to tackle the commuting congestion at train stations in major destination areas. Considering the randomness and the bias of the observed boarding/alighting demands, we proposed an improved method based on the original method to overcome the drawbacks. In this study, we exploited the properties of the transit faring model, i.e., [M2], and

utilized inexact and less information to cut the infeasible regions of a domain. The advantages of the improved algorithm lie in two aspects: First, the reliability of the proposed method is significantly enhanced. The original method relies on the actual passenger demand to identify infeasible regions. However, it is hard to estimate reliable passenger demand in the real situation. Thus, in the improved method, we bypassed this requirement and applied an alternative condition that utilizes inexact observed passenger demand to restrict the domain. Second, the scenarios used to identify the infeasible regions in the improved method are simplified which enhances the applicability. More importantly, by choosing a suitable trial point, the improved method can also achieve an exponential convergence rate. Numerical studies are performed to test the improved learning-and-optimization algorithm. The Pareto-optimal solution can be obtained rapidly, no matter the observation accuracy, and initial states. In the meantime, the convergence rate is demonstrated the same as the original method. A discrete version is also proposed to align with the real fare charging scheme.

Our proposed approach can also be extended and applied for other practical problems. For example, in many industries, firms offer product lines with multiple substitutable products (e.g, a standard-quality product and a premium-quality product) and face stochastic demands and inventory constraints. Firms can use prices to influence the demand for each product. How to change the prices to meet the inventory constrain when facing unpredictable demand? Our proposed approach can be extended to analyze this kind of situations, which we leave for future study. Moreover, one can also consider to extend the model with multiple stations (more than four stations) for future study.

Acknowledgments

This research is supported by the National Natural Science Foundation of China (grant numbers 72071173, 71771050, 71831008, 71922007), and the MOE (Ministry of Education in China) Project of Humanities and Social Sciences (Project No. 20YJAZH083).

Appendix

Appendix A. Polygons that could be generated by the improved learning-and-optimization method

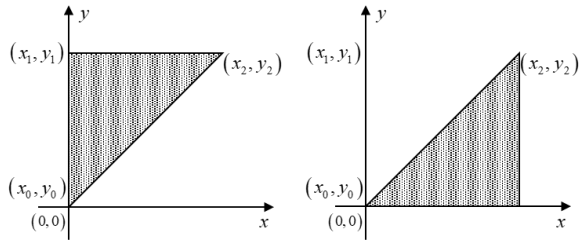

a-1 a-2

(a) Triangle

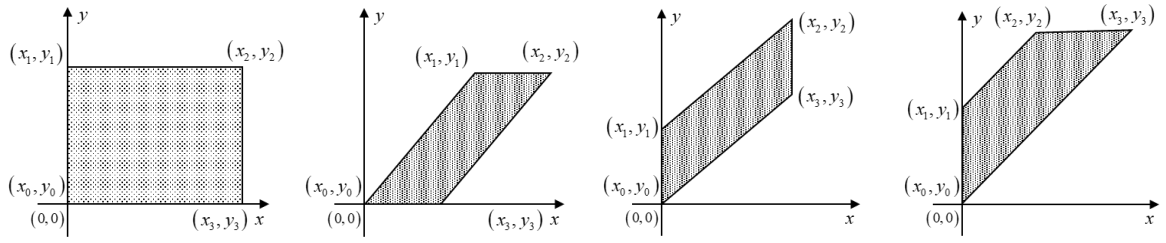

b-1 b-2 b-3 b-4

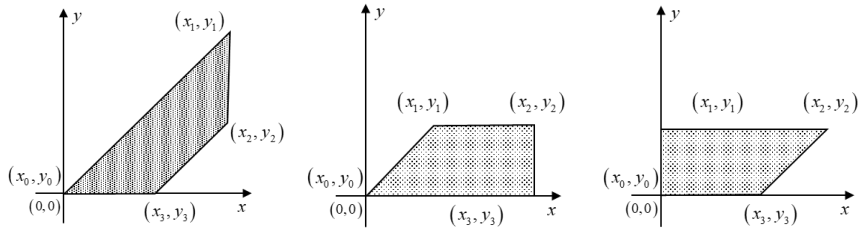

b-5 b-6 b-7

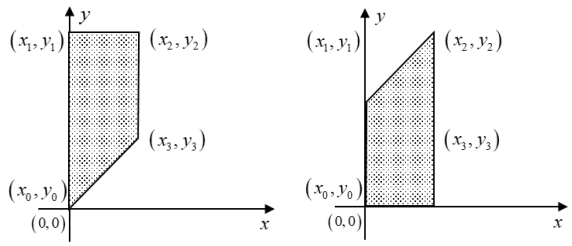

b-8 b-9

(b) Quadrangle

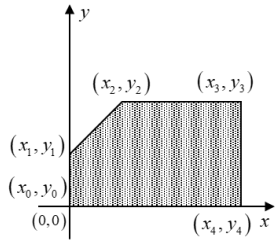

c-1

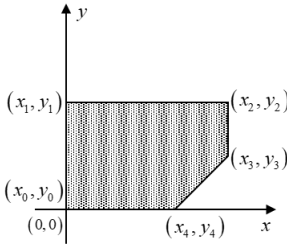

c-2

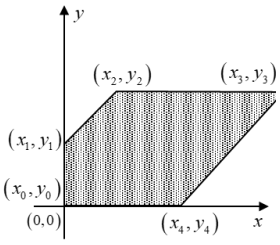

c-3

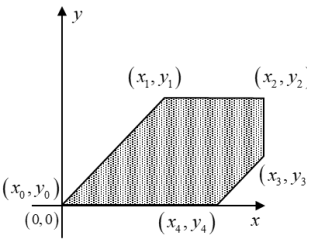

c-4

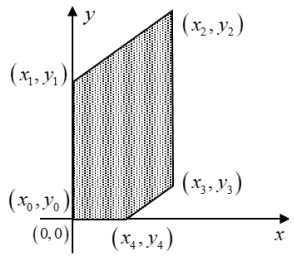

c-5

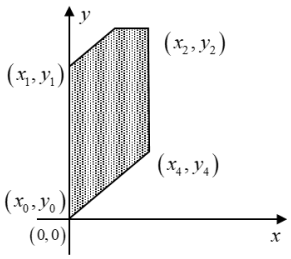

c-6

(c) Pentagon

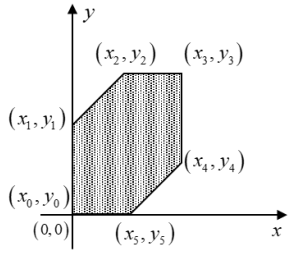

d-1

(d) Hexagon

Appendix B. Proof of Proposition 1

Proof: The initial domain $D^{(0)}$ formed by $\bar{x}$ and $\bar{y}$ is a rectangle, $[0,\bar{x}]\times[0,\bar{y}]$. Let $(x_1,y_1),(x_2,y_2)\in D^{(0)}$ (arbitrary two points in the domain) and $0\le x_1<x_2\le\bar{x}$, $0\le y_1<y_2\le\bar{y}$. Let $\lambda\in(0,1)$. We have:

$$0\le x_1=(1-\lambda)x_1+\lambda x_1<(1-\lambda)x_1+\lambda x_2<(1-\lambda)x_2+\lambda x_2=x_2\le\bar{x} \tag{17}$$

$$0\le y_1=(1-\lambda)y_1+\lambda y_1<(1-\lambda)y_1+\lambda y_2<(1-\lambda)y_2+\lambda y_2=y_2\le\bar{y}. \tag{18}$$

Eq. (17) and Eq. (18) denote that the line segment formed by (x_1, y_1) and (x_2, y_2) is a subset of the domain $[0, \bar{x}] \times [0, \bar{y}]$. Following Definitions 1 and 2, it is easy to see the initial domain is convex.

Assume the domain is still convex at the n^{th} iteration. Then, at iteration $n+1$, the restricted domain $D^{(n+1)}$ can be written as:

$$x + (y'' - x') \le y \le x + (y' - x') \tag{19}$$

$$\underline{x} \le x \le \bar{x} \tag{20}$$

$$\underline{y} \le y \le \bar{y} \tag{21}$$

where $\bar{x}$, $\underline{x}$, $\bar{y}$, $\underline{y}$, x' y', and y'' are the given parameters to form the domain, which will be repeatedly updated during iterations. Note that $\underline{x} < \bar{x}$, $\underline{y} < \bar{y}$, and $y' < y''$. Eq. (19) denotes two parallel lines with the slope of 45 degree; Eq. (20) and Eq. (21) denote two vertical and horizontal lines, respectively. Similarly, let $(x_1, y_1), (x_2, y_2) \in D^{(n+1)}$, $x_1 < x_2$, $y_1 < y_2$, $\lambda \in (0,1)$. We have:

$$\begin{aligned} x_1 + (y'' - x') \le y_1 &= (1-\lambda) y_1 + \lambda y_1 < (1-\lambda) y_1 + \lambda y_2 \\ &< (1-\lambda) y_2 + \lambda y_2 = y_2 \le x_2 + (y' - x') \end{aligned} \tag{22}$$

$$\begin{aligned} \underline{x} \le x_1 &= (1-\lambda) x_1 + \lambda x_1 < (1-\lambda) x_1 + \lambda x_2 \\ &< (1-\lambda) x_2 + \lambda x_2 = x_2 \le \bar{x} \end{aligned} \tag{23}$$

$$\begin{aligned} \underline{y} \le y_1 &= (1-\lambda) y_1 + \lambda y_1 < (1-\lambda) y_1 + \lambda y_2 \\ &< (1-\lambda) y_2 + \lambda y_2 = y_2 \le \bar{y} \end{aligned} \tag{24}$$

Eq. (22)–(24) denote the line segment formed by (x_1, y_1) and (x_2, y_2) is a subset of the domain $D^{(n+1)}$. According to Definitions 1 and 2, the domain $D^{(n+1)}$ is convex.

□

References

Australian Bureau of Statistics, 2018. Census of population and housing. https://www.abs.gov.au/ausstats/abs@.nsf/Lookup/by%20Subject/2071.0.55.001~2016~Main%20Features~Feature%20Article:%20Journey%20to%20Work%20in%20Australia~40. Accessed January 2020.

Bourke, P., 1988. Calculating the area and centroid of a polygon. https://www.seas.upenn.edu/~sys502/extra_materials/Polygon%20Area%20and%20Centroid.pdf. Accessed January 2020.

Boyd, S., Vandenberghe, L., 2004. *Convex optimization*. Cambridge university press, Cambridge, U.K.

Chu, C.-W., Hsu, H.-L., 2019. A heuristic algorithm for multiple trip vehicle routing problems with time window constraint and outside carrier selection. *Maritime Business Review* 4(3), 256-273.

Currie, G., 2011. Design and impact of a scheme to spread peak rail demand using pre-peak free fares, *European Transport Conference 2011*, Glasgow, United Kingdom.

Douglas, N.J., Henn, L., Sloan, K., 2011. Modelling the ability of fare to spread AM peak passenger loads using rooftops, *34th Australasian Transport Research Forum*, Adelaide, Australia.

Downs, A., 1993. Point of view: implementing peak-hour road pricing at fullscale: finding solutions to practical problems. *TR News* 167, 7-9.

Gao, K., Yang, Y., Sun, L., Qu, X., 2020. Revealing psychological inertia in mode shift behaviorand its quantitative influences on commuting trips. *Transportation Research Part F: Traffic Psychology and Behaviour* 71, 272–287.

Guo, R., Yang, H., Huang, H., Tan, Z., 2015. Day-to-day flow dynamics and congestion control. *Transportation Science* 50(3), 982-997.

Guo, X., Xu, D., 2016. Profit maximization by a private toll road with cars and trucks. *Transportation Research Part B: Methodological* 91, 113-129.

Han, D., Xu, W., Yang, H., 2010. Solving a class of variational inequalities with inexact oracle operators. *Mathematical Methods of Operations Research* 71(3), 427-452.

Han, D., Yang, H., 2009. Congestion pricing in the absence of demand functions. *Transportation Research Part E: Logistics and Transportation Review* 45(1), 159-171.

Ho, J.D., Bernal, P., 2019. Panama Canal vs alternative routes: estimating a logit model for grains. *Maritime Business Review* 5(1), 99-120.

Kavoosi, M., Dulebenets, M.A., Abioye, O., Pasha, J., Theophilus, O., Wang, H., Kampmann, R., Mikijeljević, M., 2019. Berth scheduling at marine container terminals. *Maritime Business Review* 5(1), 30-66.

Li, M.Z.F., 2002. The role of speed-flow relationship in congestion pricing implementation with an application to Singapore. *Transportation Research Part B: Methodological* 36(8), 731-754.

Liu, Z., Zhang, Y., Wang, S., Li, Z., 2017. A trial-and-error method with autonomous vehicle-to-infrastructure traffic counts for cordon-based congestion pricing. *Journal of Advanced Transportation* 2017, 1-8.

Meng, Q., Liu, Z., 2011. Trial-and-error method for congestion pricing scheme under side-constrained probit-based stochastic user equilibrium conditions. *Transportation* 38(5), 819-843.

Meng, Q., Xu, W., Yang, H., 2005. Trial-and-error procedure for implementing a road-pricing scheme. *Transportation Research Record* 1923(1), 103-109.

Qu, X., Yu, Y., Zhou, M., Lin, C.-T., Wang, X., 2020. Jointly dampening traffic oscillations and improving energy consumption with electric, connected and automated vehicles: A reinforcement learning based approach. *Applied Energy* 257, 114030.

Vickrey, W.S., 1993. Point of view: principles and applications of congestion pricing. *TR News* 167, 4-5.

Wang, S., Zhang, W., Qu, X., 2018. Trial-and-error train fare design scheme for addressing boarding/alighting congestion at CBD stations. *Transportation Research Part B: Methodological* 118, 318–335.

Wang, X., Yang, H., 2012. Bisection-based trial-and-error implementation of marginal cost pricing and tradable credit scheme. *Transportation Research Part B: Methodological* 46(9), 1085-1096.

Wang, X., Yang, H., Han, D., Liu, W., 2014. Trial and error method for optimal tradable credit schemes: The network case. *Journal of Advanced Transportation* 48(6), 685-700.

Wu, J., Kulcsár, B., Ahn, S., Qu, X., 2020. Emergency vehicle lane pre-clearing: From microscopic cooperation to routing decision making. *Transportation Research Part B: Methodological* 141, 223–239.

Xu, M., Meng, Q., Huang, Z., 2016. Global convergence of the trial-and-error method for the traffic-restraint congestion-pricing scheme with day-to-day flow dynamics. *Transportation Research Part C: Emerging Technologies* 69, 276-290.

Xu, Y., Zheng, Y., Yang, Y., 2021. On the movement simulations of electric vehicles: A behavioral model-based approach. *Applied Energy* 283, 116356.

Yang, H., Huang, H., 2005. *Mathematical and Economic Theory of Road Pricing*. Elsevier, Oxford, United Kingdom.

Yang, H., Meng, Q., Lee, D., 2004. Trial-and-error implementation of marginal-cost pricing on networks in the absence of demand functions. *Transportation Research Part B: Methodological* 38(6), 477-493.

Yang, H., Xu, W., He, B., Meng, Q., 2010. Road pricing for congestion control with unknown demand and cost functions. *Transportation Research Part C: Emerging Technologies* 18(2), 157-175.

Yang, H., Xu, W., Meng, Q., 2005. A sequential experimental approach for analyzing second-best road pricing with unknown demand functions, *16th International Symposium on Transportation and Traffic*, Maryland, United States.

Ye, H., Yang, H., Tan, Z., 2015. Learning marginal-cost pricing via a trial-and-error procedure with day-to-day flow dynamics. *Transportation Research Part B: Methodological* 81, 794-807.

Zhou, B., Bliemer, M., Yang, H., He, J., 2015. A trial-and-error congestion pricing scheme for networks with elastic demand and link capacity constraints. *Transportation Research Part B: Methodological* 72, 77-92.

Zhou, B., Xu, M., Zhang, Y., 2019. A trial-and-error congestion pricing method for day-to-day dynamic network flows considering travelers' heterogeneous inertia patterns. *Mathematical Problems in Engineering* 2019, 1-17.